IEEE Photonics Journal
An IEEE Photonics Society Publication

Invited Paper

Refractive Index Engineering With Subwavelength Gratings in Silicon Microphotonic Waveguides

Volume 3, Number 3, June 2011

J. H. Schmid
P. Cheben
P. J. Bock
R. Halir
J. Lapointe
S. Janz
A. Delâge
A. Densmore
J.-M. Fédeli
T. J. Hall
B. Lamontagne
R. Ma
I. Molina-Fernández
D.-X. Xu

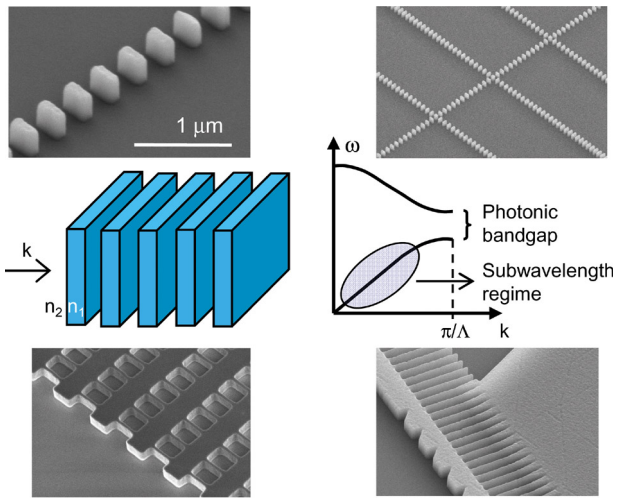

DOI: 10.1109/JPHOT.2011.2139198
1943-0655/$26.00 ©2011 IEEE

IEEE photonics SOCIETY

IEEE

Refractive Index Engineering With Subwavelength Gratings in Silicon Microphotonic Waveguides

J. H. Schmid,[1] P. Cheben,[1] P. J. Bock,[1] R. Halir,[2] J. Lapointe,[1] S. Janz,[1] A. Delâge,[1] A. Densmore,[1] J.-M. Fédeli,[3] T. J. Hall,[4] B. Lamontagne,[1] R. Ma,[1] I. Molina-Fernández,[2] and D.-X. Xu[1]

(Invited Paper)

[1]Institute for Microstructural Sciences, National Research Council Canada, Ottawa, ON K1A 0R6, Canada
[2]Departamento Ingeniería de Comunicaciones, ETSI Telecomunicacíon, Universidad de Málaga, 29071 Málaga, Spain
[3]CEA-LETI, Minatec, CEA-Grenoble, 38054 Grenoble, France
[4]Centre for Research in Photonics, University of Ottawa, Ottawa, ON K1N 6N5, Canada

DOI: 10.1109/JPHOT.2011.2139198

Manuscript received February 28, 2011; revised March 28, 2011; accepted March 28, 2011. Date of current version June 28, 2011. Corresponding author: J. H. Schmid (e-mail: Jens.Schmid@nrc-cnrc.gc.ca).

Abstract: In this review, we summarize and discuss our recent studies of subwavelength grating (SWG) structures for engineering the refractive index of silicon microphotonic waveguides. The SWG effect allows control of the effective refractive index of a waveguide core over a range spanning the values of the cladding material and silicon by lithographic patterning. We demonstrate this effect with the example of segmented photonic wire waveguides, which are shown to exhibit low propagation loss, and can be used to make highly efficient waveguide crossings and in-plane fiber–chip coupling structures. Other applications of SWG structures in silicon photonic waveguide devices include surface grating couplers with enhanced performance and simplified fabrication requirements, as well as a novel curved waveguide sidewall grating microspectrometer, in which an SWG structure fulfills a dual purpose by acting as an effective slab waveguide for diffracted light and as a lateral cladding for a channel waveguide.

Index Terms: Silicon photonics, nanophotonics, subwavelength gratings (SWGs), waveguides.

1. Introduction

Diffraction effects are suppressed for light propagating through dielectric grating structures with a periodicity smaller than one half of the wavelength of light. The use of such subwavelength gratings (SWGs) is well established in free space optics [1]. It is known that SWGs act as homogeneous effective media with spatially averaged refractive index [2]. They have found applications, for example, as an alternative to antireflective (AR) optical thin film coatings on bulk dielectric surfaces [3]. We have previously demonstrated that this AR effect can also be used on planar optical waveguide facets [4]. The case of a 1-D SWG is illustrated in Fig. 1(a). The structure is comprised of alternating slabs of dielectric materials with refractive indices n_1 and n_2 with a periodicity $\Lambda < \lambda/2$. For the case of light incident on the grating from the top in Fig. 1(a), the effective index of the SWG depends on the polarization of the light. According to the effective medium theory (EMT), the

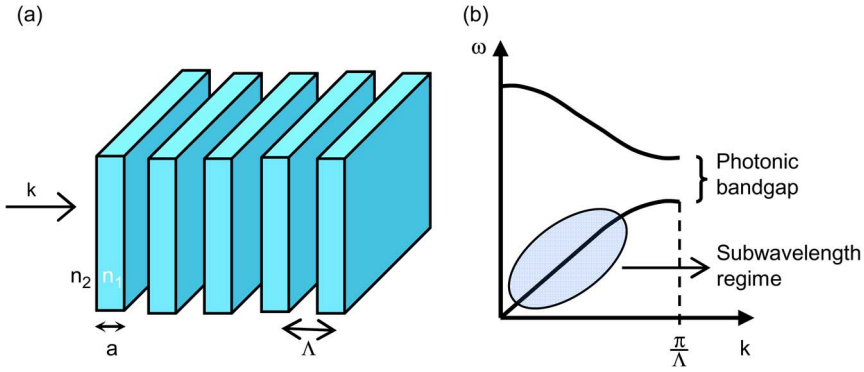

Fig. 1. (a) Schematic picture of a subwavelength grating (SWG) consisting of alternating slabs of dielectric materials with indices n_1 and n_2, with pitch Λ, and duty ratio a/Λ. (b) Dispersion diagram of light propagating through the periodic structure, indicating the photonic bandgap and the subwavelength region.

effective refractive index is given by $n_{\parallel} = (fn_1^2 + (1-f)n_2^2)^{1/2}$ and $n_{\perp} = (fn_1^{-2} + (1-f)n_2^{-2})^{-1/2}$ for a wave with the electric field parallel and perpendicular to the slabs, respectively, where $f = a/\Lambda$ is the volume fraction of the material with index n_1. The effective index is thus a polarization dependent weighted average of the indices of the constituent materials. The optical properties of the same structure for light incident perpendicular to the dielectric slabs with wave vector k, are well-known from the study of photonic crystals [5]. Light propagates through the periodic structure as a Bloch wave with a dispersion relation that looks schematically as depicted in Fig. 1(b). At the Bragg condition $k = \pi/\Lambda$, the slope of the dispersion curve vanishes, corresponding to a standing wave with a group velocity of zero, and a band of forbidden frequencies exists: the "photonic band gap." A great deal of experimental work has focused on exploiting the photonic band gap effect for making optical waveguides, cavities and related device structures. SWGs, on the other hand, operate in the long wavelength regime of the dispersion diagram, as indicated in Fig. 1(b), where dispersion is approximately linear, consistent with the concept of an effective homogeneous medium.

The spatial averaging effect of SWGs introduces a new degree of freedom in the design of integrated photonic circuits, where the refractive index contrast is otherwise set by the choice of the material platform. For example, for silicon photonic circuits operating at a wavelength near $\lambda = 1.55$ μm, the waveguide core and the cladding indices are given by the material constants of silicon $(n = 3.5)$ and silicon dioxide $(n = 1.44)$, and waveguide devices are generally designed within the constraint of these fixed values. We have recently demonstrated that the refractive index of the waveguide core medium can be modified locally with SWGs. Importantly, our method only relies on standard fabrication techniques and can be implemented with no modifications to the chip fabrication process flow. In this review, we will discuss various applications of refractive index engineering in silicon photonic circuits, namely, SWG waveguide crossings, tapered fiber–chip couplers, and SWG structures for vertical grating couplers and novel optical waveguide spectrometers.

2. SWG Waveguides

A basic building block of silicon photonic waveguide devices is the photonic wire waveguide: a single-mode silicon channel waveguide with typical cross sections of approximately 500 nm in width and 200–300 nm in height. These waveguides exhibit low loss for bends with radii as small as a few micrometers, thus facilitating device miniaturization. They are also used in remarkably sensitive chemical or biological evanescent field sensors [6]. The structure shown in Fig. 2(a) exemplifies refractive index engineering of a silicon photonic wire waveguide using the SWG spatial averaging effect. By etching periodic gaps of a well defined breadth b and pitch Λ into a standard silicon photonic wire, an SWG waveguide is formed with an effective core index determined by the duty

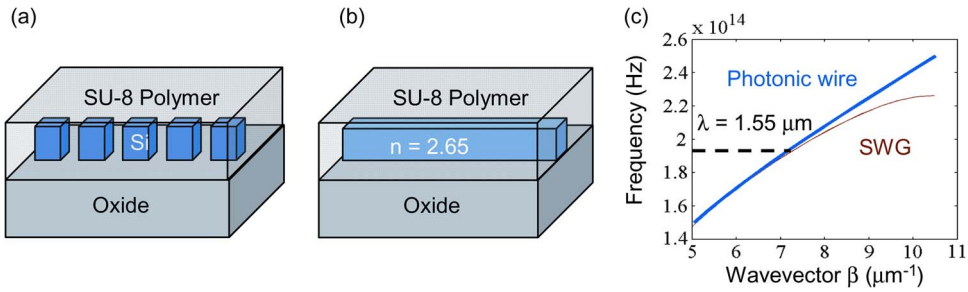

Fig. 2. (a) Schematic picture of a silicon SWG waveguide. (b) Equivalent effective wire waveguide with a spatially averaged core refractive index. (c) Calculated dispersion diagrams of the structures shown in (a) and (b) (TE polarization) showing a good match for the operating wavelength of 1.55 μm.

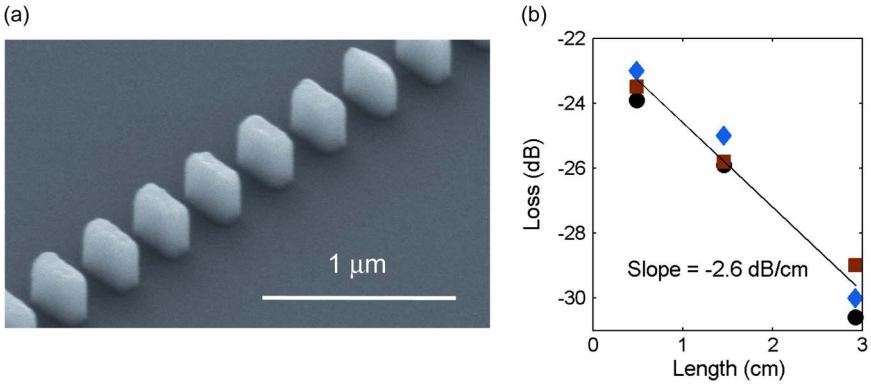

Fig. 3. (a) Scanning electron micrograph of a fabricated SWG waveguide. (b) Measured waveguide transmission loss as a function of straight waveguide length (three data sets) and linear fit yielding a propagation loss of 2.6 dB/cm for the TE mode.

ratio $1 - b/\Lambda$. We expect that the optical properties of the structure shown in Fig. 2(a) should be similar to the one shown in Fig. 2(b), namely a photonic wire waveguide of identical cross section but with a reduced refractive index value of the waveguide core. This is theoretically confirmed by superimposing the calculated dispersion curves of the two structures, as depicted in Fig. 2(c) for a waveguide cross section of 0.45 μm $\times$ 0.26 μm and an SWG duty ratio of 50%. The SWG waveguide dispersion, which is calculated using the freely available MIT photonics band software, exhibits the typical behavior expected for a periodic waveguide with a flattening of the dispersion at the Bragg condition (at $\beta_{\text{Bragg}} = 10.5\ \mu\text{m}^{-1}$). Near the operating wavelength of $\lambda = 1.55\ \mu$m, which lies in the subwavelength regime of the diagram as indicated in the figure, there is a good match between dispersions of the SWG waveguide and the effective photonic wire with a core index of $n = 2.65$. In both cases, the transverse-electric (TE) mode is plotted.

Experimentally, we have fabricated SWG waveguides from commercial silicon-on-insulator (SOI) substrates with 0.26-μm-thick silicon and 2-μm-thick buried oxide (BOX) layers. We used electron beam lithography and inductively coupled plasma reactive ion etching (ICP-RIE) with a mixture of SF_6 and C_4F_8 gases to make the waveguide structures. The nominal width of the silicon segments was 300 nm, their length 150 nm, and the grating period was 300 nm, corresponding to a duty cycle of 50%. As the upper cladding layer we applied a 2-μm-thick SU-8 polymer layer by a standard spin and bake procedure. A scanning electron microscope (SEM) image of a fabricated SWG waveguide is shown in Fig. 3(a). Due to a bias in the fabrication process, the width and duty cycle of the fabricated SWG structure are approximately 250 nm and 33%, respectively.

We estimated the propagation loss by measuring the power transmitted through straight SWG waveguides of 5, 15, and 30 mm length. For these measurements, we used a lensed polarization

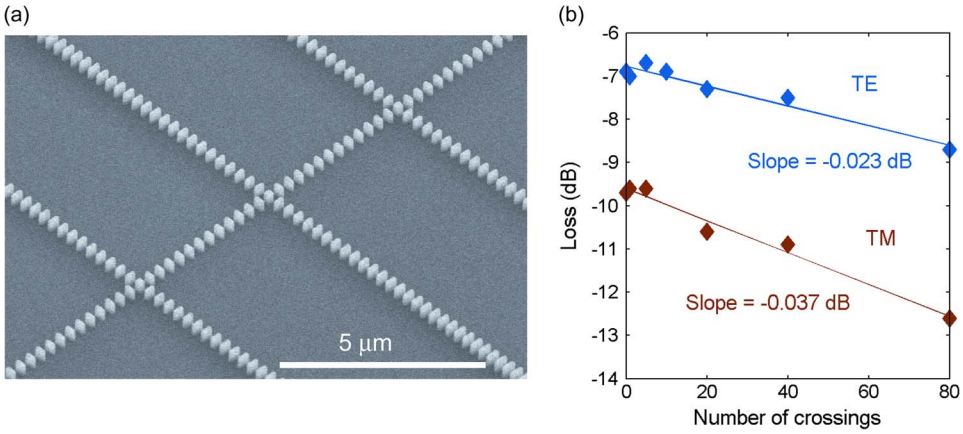

Fig. 4. (a) Scanning electron micrograph of three concatenated SWG waveguide crossings. (b) Measured transmission loss of concatenated crossing structures as a function of the number of crossings with linear fits.

maintaining optical fiber to couple light from a broadband amplified spontaneous emission (ASE) source with a 3-dB wavelength range from 1530 to 1560 nm into the waveguides and an InGaAs photodetector to measure the output intensity. Three data sets of loss as a function of waveguide length are plotted in Fig. 3(b). The linear fit to the transmission data yields a typical propagation loss of 2.6 dB/cm for the TE mode with a polarization dependent loss (PDL) of less than 0.5 dB/cm [7], the losses of the transverse-magnetic (TM) mode being slightly greater than the corresponding TE losses. At first sight, these loss values, which are comparable to the best photonic wire waveguides reported, appear surprisingly low, considering that the light has to propagate through more than 30 000 high-index contrast discontinuities per centimeter in an SWG waveguide. However, according to Bloch theory, the ideal periodic waveguide structure, as shown in Fig. 2(a), should, in principle, be lossless. We believe that the propagation loss originates predominately from light scattering at the rough interfaces of the fabricated structure, as is the case for standard photonic wire waveguides. For our SWG waveguides, which have nominally a periodicity equal to the width and 50% duty ratio, the total area of scattering interfaces per unit length is equal to the sidewall area of a photonic wire waveguide. This is consistent with an observed scattering loss of comparable magnitude for the two waveguide types. A theoretical treatment of scattering losses similar to the analysis of channel waveguides [8], based on the standard Payne-Lacey model of slab waveguides [9], is still outstanding for SWG waveguides.

An interesting application of SWG waveguides is waveguide crossings, such as the ones shown in the SEM image in Fig. 4(a). The ability to intersect waveguides with low loss and crosstalk is often considered to be a prerequisite for designing complex high-density photonic circuits. Previous designs of photonic wire crossings have made use of a double etch structure, widening the channel to ridge waveguides in the crossing area [10], and shape optimization of the wire crossing with a genetic algorithm [11]. In both cases, crossing losses in the range of 0.1–0.2 dB with crosstalk of -40 dB or better were demonstrated for TE polarized light. As discussed above, the core refractive index of SWG waveguides is, according to EMT, reduced, compared with a silicon wire waveguide, and thus, the optical properties of the segmented waveguides are similar to a lower index-contrast system. This is advantageous for the design of crossings for two reasons. First, a waveguide crossing over another presents a lesser perturbation in a low index contrast system than in a high-index contrast system, and therefore, scattering and diffraction losses at the crossing point are reduced. Second, the effectively low index contrast of an SWG waveguide leads to a more delocalized mode profile compared to a photonic wire waveguide of identical cross section. The overlap of a delocalized SWG waveguide mode with the index perturbation presented by the waveguide that is being intersected is smaller than that of the more confined mode of a wire waveguide. We determined the loss per SWG waveguide crossing experimentally by measuring the transmission

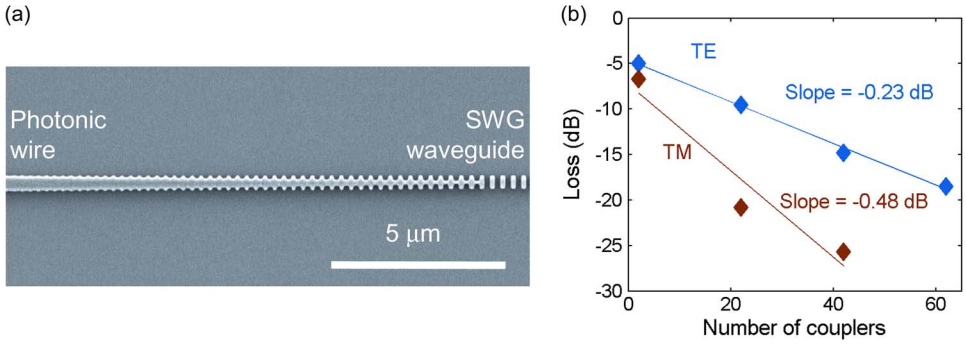

Fig. 5. (a) Scanning electron micrograph of SWG to photonic wire coupling structure. (b) Measured transmission loss of concatenated coupling structures as a function of the number of couplers with linear fits.

loss of concatenated structures, as seen in Fig. 4(a) for a variable number of serial crossings with optimized grating parameters [12]. The resulting plots of loss as a function of the number of crossings are shown in Fig. 4(b). Loss per crossing was determined from a linear fit to the data to be -0.023 dB and -0.037 dB for TE and TM polarized light, respectively, with a crosstalk better than -40 dB. These results confirm impressively the suitability of SWG waveguides for designing highly efficient crossings.

SWG waveguides and photonic wire waveguides can be integrated on a chip, and one type of waveguide can be transformed into the other using an adiabatic coupler structure, as shown in Fig. 5(a). The operating principle of the coupler is a gradual modification of the effective index along its length to match the photonic wire waveguide on one end and the SWG waveguide on the other. This is achieved by chirping the grating period and duty cycle. Towards the photonic wire side, we also use bridge elements of linearly increasing width inside the gaps of the segmented waveguide over a distance of 13 μm. In this region, the coupler is essentially a photonic wire waveguide with a subwavelength sidewall grating. The total length of the coupler from a 450-nm-wide photonic wire to a 300-nm-wide SWG waveguide with a duty ratio of 50% is 50 μm. We have characterized the intrinsic loss of our coupler structure by measuring transmittance of waveguides with a variable number of concatenated couplers, up to a maximum of 64. The resulting curve of loss as a function of the number of couplers is shown in Fig. 5(b). From the linear fit, the intrinsic coupler loss of 0.23 dB for TE polarized light and 0.48 dB for TM is obtained [13].

In addition to enabling the seamless integration of wire and SWG waveguides on a chip, essentially the same structure can be used for making highly efficient photonic wire fiber–chip couplers. Such couplers were originally proposed in [14]. In this case, the SWG waveguide is extended to the chip edge, where it is coupled to a lensed single-mode fiber with a Gaussian beam waist of 2 μm. We have found that the coupling efficiency is optimized for a SWG waveguide width of 350 nm, a period of 400 nm and a duty ratio of 50%. For these parameters, from measured insertion loss and taking into account the waveguide propagation loss and the intrinsic coupler loss, we estimate the total fiber to waveguide coupling efficiency to be -0.9 dB for TE and -1.2 dB for TM polarization. We have also found that the couplers are remarkably robust against changes in the SWG waveguide width, with a negligible loss contribution of -0.1 dB for a 50-nm width reduction. These results constitute a marked improvement in both coupling efficiency and fabrication tolerance over photonic wire inverse taper structures [15], which are typically used for in-plane fiber–chip coupling to photonic wires.

3. SWG Structures for Grating Couplers and Microspectrometers

Another common way of coupling light from an optical fiber to a silicon photonic wire waveguide is by means of a diffraction grating. In this case, the optical fiber is brought into proximity to the waveguide surface, which is patterned with the grating, from the top, typically at a near-normal

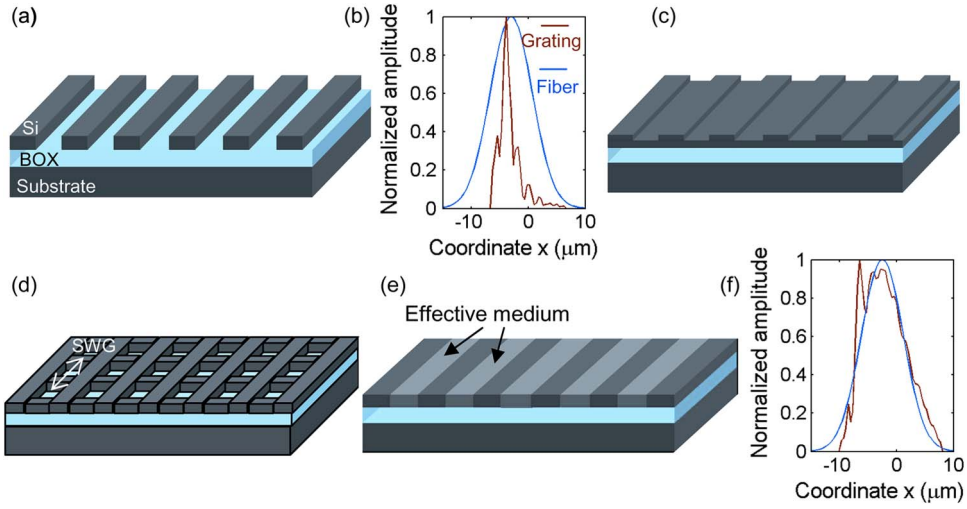

Fig. 6. (a) Schematic picture of a fully etched silicon surface grating coupler. (b) Comparison of beam profiles of diffracted beam from the fully etched grating shown in (a) with the Gaussian profile of a single-mode optical fiber. (c) Partially etched grating with reduced coupling strength. (d) Fully etched grating incorporating lateral SWG structure inside the grating grooves. (e) Equivalent structure with grooves filled by an effective dielectric medium. (f) Calculated beam profile of diffracted beam from an optimized apodized grating with SWG structures as in (d) compared to single-mode fiber beam profile.

angle. Grating couplers can be efficient, relatively easy to fabricate, eliminate the need for polished waveguide facets, and make wafer scale testing of devices possible. The simplest grating coupler structure that can be used is depicted in Fig. 6(a), in which the grating grooves are etched all the way through the silicon waveguide layer down to the BOX. This structure can readily be fabricated in a single etch that also defines the waveguide pattern. Due to the high-index contrast of the silicon and cladding layers, it is a strong grating with a short coupling length. This means that light propagating through the waveguide into the grating area is diffracted toward the optical fiber over a short distance on the order of only a few micrometers. The resulting profile of the diffracted beam is much narrower than the mode diameter of a standard single-mode fiber, as shown in Fig. 6(b). The calculated mode overlap is 35%, which limits the coupling efficiency. The situation can be improved by using a weaker grating. An obvious way to reduce the grating strength is to etch the grooves only partially through the silicon layer, as shown in Fig. 6(c). Coupling efficiency for the partially etched structures is significantly improved [16], [17]; however, a more complex fabrication process with an additional etch step, requiring good etch depth control and uniformity, is required.

To circumvent this problem, it has been proposed that SWG structures can be used inside the grating grooves to effectively reduce the index contrast of a fully etched grating [18]. The structure is shown schematically in Fig. 6(d). Due to the spatial averaging effect of the SWG, the grooves are filled in with an effective medium with an index determined by the duty ratio of the SWG structure, as depicted in Fig. 6(e). The index contrast and, thus, the grating strength can be modified spatially simply by varying the SWG duty ratio. This makes it straightforward to introduce grating apodization to maximize the overlap of the diffracted beam with the fiber mode. Fig. 6(f) shows the fiber mode and diffracted beam profiles for an optimized apodized coupling structure with a calculated overlap of 94%.

The SEM images in Fig. 7(a)–(d) show fabricated grating couplers without and with apodization. Couplers were designed for TM polarized light, as required for compatibility with our evanescent field sensors [6]. They were fabricated with the same process described above for the SWG waveguides, using electron beam lithography. Coupling efficiency was estimated from the insertion loss of two couplers connected back to back, subtracting the propagation loss of the connecting silicon wire waveguide. Experimental results for coupling efficiency of the uniform and the apodized

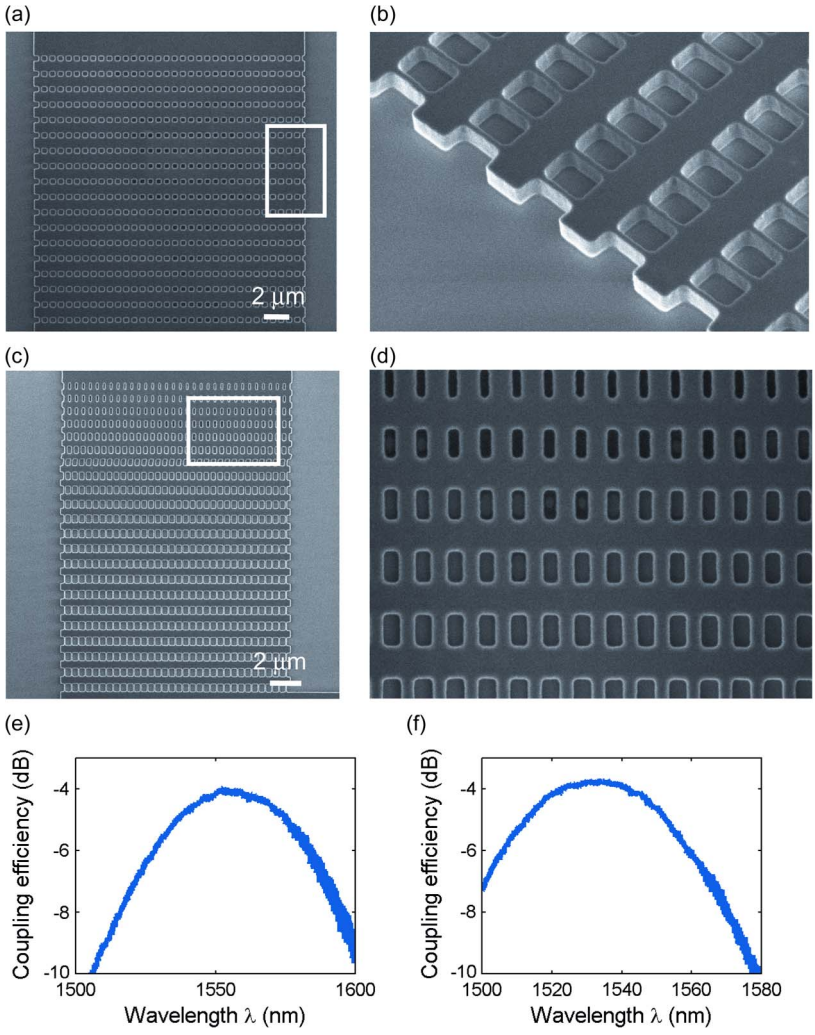

Fig. 7. (a) SEM micrograph of a grating coupler with uniform SWG structure. (b) Magnified view of the area marked by the white box in (a). (c) Apodized SWG grating coupler. (d) Magnified view showing the changing duty ratio of the SWG structure for each row of the grating. (e) Measured coupling efficiency curve for a uniform coupler. (f) Coupling efficiency for the apodized grating coupler.

grating as a function of wavelength are shown in Fig. 7(e) and (f), respectively, with peak efficiencies of 4 dB and 3.7 dB and 3-dB-bandwidths of approximately 60 nm [19]. These values are in good agreement with FDTD simulations, although the efficiency improvement achieved by apodization was found to be slightly less than theoretically expected. Although the results shown here were obtained for gratings fabricated by electron beam lithography, the grating structures shown in Fig. 7 employ SWGs with a pitch of 450 nm and a minimum feature size of 100 nm, which is compatible with the resolution of deep-UV (DUV) lithography systems. Devices have in fact been successfully fabricated with DUV lithography on 8-in wafers at LETI with comparable coupling efficiencies. Finally, recent experimental studies confirm that, as one might expect, the principle of grating strength optimization with SWG structures is also applicable to couplers optimized for TE polarized light [20], [21], which is more commonly used in silicon photonic wire devices. Reported coupling efficiencies for TE polarization are similar to our TM couplers. Subwavelength binary blazed grating couplers have been discussed in the literature for applications as beam splitters [22], [23].

As demonstrated in the previous examples, SWGs make it possible to control the refractive index of a waveguide in a specific location on a chip. This control is also possible for slab waveguides. We

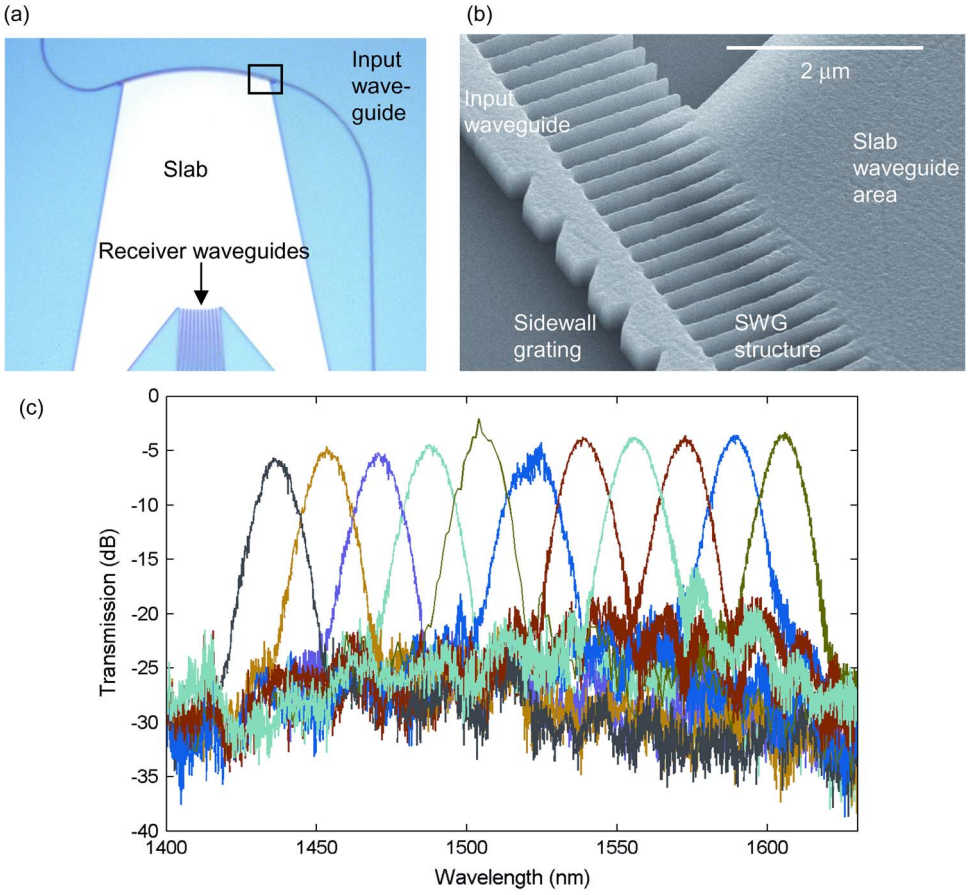

Fig. 8. (a) Optical micrograph of a curved waveguide sidewall grating spectrometer device incorporating an SWG nanostructure. (b) SEM micrograph of the SWG, which acts simultaneously as an effective slab waveguide for diffracted light and as a lateral waveguide cladding for the channel waveguide, in the trench between the input and the slab waveguide area structure, as marked by the box in (a). (c) Measured transmission spectra for 11 channels of the spectrometer.

have made use of this fact in our design of a novel curved waveguide sidewall grating spectrometer. An optical micrograph of a fabricated device is shown in Fig. 8(a). In this spectrometer, light entering the device through the input photonic wire waveguide is diffracted by a waveguide sidewall grating into a slab waveguide region. Direction of the diffracted light is at an angle of 90° to the waveguide for the center wavelength. Angular dispersion as a function of wavelength is used to attain spectral separation. The input waveguide is curved in the grating region to focus the diffracted light in a curved plane of the slab that is intercepted by the output photonic wire waveguides. The function of this spectrometer has been explained in more detail in [24]. In order to couple the diffracted light from the sidewall grating to the slab waveguide region efficiently, an SWG structure is implemented in the trench between the input and slab waveguides. This structure can be seen in the SEM micrograph in Fig. 8(b). Near the wire waveguide, the SWG trench acts as an effective slab waveguide with a reduced effective core index for light diffracted by the grating toward the combiner region, as well as a lateral cladding for the strip waveguide. On the other side of the trench, near the slab waveguide combiner, a triangular SWG structure is used as a graded-index medium to suppress Fresnel reflection for the light propagating from the trench to the slab waveguide, which is similar to the AR structures in [4]. In Fig. 8(c), we present transmission spectra for 11 channels of the spectrometer. The measured extinction ratio is as large as 20 dB, and the loss is approximately -4 dB, demonstrating the efficiency of light coupling through the SWG region. The device has a wavelength bandwidth of 170 nm for a device size of only $\sim 160\ \mu\text{m} \times 100\ \mu\text{m}$ [13].

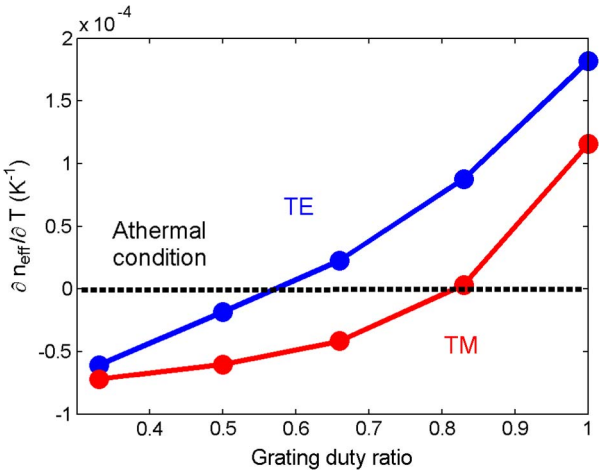

Fig. 9. Calculated thermooptic coefficient of an SWG waveguide with SU-8 polymer cladding as a function of the grating duty ratio, demonstrating that athermal behavior can be achieved for duty ratios of ~58% and 82% for TE and TM polarized light, respectively.

4. Conclusion and Future Directions

In this review, we have discussed a number of examples of refractive index engineering by SWG structures for planar waveguide devices. The SWG effect can be used to modify the core index of photonic wire waveguides, which are a basic building block of silicon integrated photonic circuits. The resulting SWG waveguides exhibit low propagation losses on the order of 2–3 dB/cm and can be used to design highly efficient waveguide crossings with losses as low as −0.02 dB and negligible crosstalk. One can envision a multitude of other applications of SWG waveguides. For example, subwavelength segmentation allows one to control the relative overlap of the optical mode with the waveguide core and cladding materials. In particular, it is often desirable to increase the overlap with the cladding material beyond the values obtained in a photonic wire waveguide. The relatively large overlap of the TE mode in slot waveguides with the filling material of the slot, for example, has been used to achieve enhanced nonlinear optical effects [25]. It appears that SWG waveguides could be used to a similar effect. Mode profile engineering can also be applied to alleviate or cancel the strong temperature dependence of silicon waveguides, thus relaxing the requirements for temperature control of devices. It has already been demonstrated that the temperature dependence of silicon wire waveguides can be reduced by using a polymer overcladding with a negative thermooptic coefficient to compensate for the large silicon thermooptic effect [26], [27]. In order to achieve athermal operation of waveguides, the overlap of the mode with the polymer cladding must be sufficient to compensate for the thermal contribution of the silicon core. We have carried out first calculations of the thermooptic constant of SWG waveguides clad with SU-8 polymer as a function of grating duty ratio. In Fig. 9, we plot dn_{eff}/dT as a function of the duty ratio of an SWG waveguide with a cross section of 0.45 μm $\times$ 0.26 μm and a period of 0.3 μm. A transition from positive to negative thermooptic constants is observed as the duty cycle is lowered by increasing the gap size and, thus, increasing the volume fraction of SU-8 polymer with a negative thermooptic material constant. The observed zero-crossing demonstrates theoretically the feasibility of designing athermal silicon SWG waveguides.

We have demonstrated adiabatic SWG to photonic wire waveguide coupling structures with loss of −0.23 dB for TE and −0.48 dB for TM polarization, which enable seamless integration of the two waveguide types on a chip. A similar structure can be employed as an in-plane fiber–chip coupler featuring high coupling efficiencies on the order of −1 dB and good fabrication tolerances, in particular to waveguide width fluctuations. SWG structures were also shown to be suitable for improving the performance and simplifying the fabrication of out-of-plane grating fiber–chip coupling structures. Here, the SWG is used to fill the grooves of the diffraction grating with an effective

medium, allowing spatial modification of the grating strength. Finally, we reviewed the operation principle and experimental results of a novel microspectrometer device, in which an SWG structure acts simultaneously as a lateral waveguide cladding and as an effective slab waveguide for diffracted light. Engineering the refractive index of slab waveguides with SWGs may also prove to be a suitable method of adapting to integrated optics components such as lenses or transmission gratings, which are common in free space optics. An example of a waveguide lens has recently been discussed in the literature [28]. The functionality and performance we have achieved for the devices and components discussed in this review suggests that refractive index engineering by SWG structures has the potential to become an important and widespread technique in the design of integrated photonic circuits.

References

[1] "Selected papers on subwavelength diffractive optics," in *SPIE Milestone Series*, J. N. Mait and D. W. Prather, Eds. Bellingham, WA: SPIE Opt. Eng. Press, 2001.

[2] S. M. Rytov, "Electromagnetic properties of a finely stratified medium," *Sov. Phys. JETP 2*, vol. 2, no. 3, pp. 466–475, 1956.

[3] H. Kikuta, H. Toyota, and W. Yu, "Optical elements with subwavelength structured surfaces," *Opt. Rev.*, vol. 10, no. 2, pp. 63–73, 2003.

[4] J. H. Schmid, P. Cheben, S. Janz, J. Lapointe, E. Post, and D.-X. Xu, "Gradient-index antireflective subwavelength structures for planar waveguide facets," *Opt. Lett.*, vol. 32, no. 13, pp. 1794–1796, Jul. 2007.

[5] J. D. Joannopoulos, S. G. Johnson, J. N. Winn, and R. D. Meade, *Photonic Crystals: Molding the Flow of Light* , 2nd ed. Princeton, NJ: Princeton Univ. Press, 2008.

[6] A. Densmore, D.-X. Xu, S. Janz, P. Waldron, T. Mischki, G. Lopinski, A. Delâge, J. Lapointe, P. Cheben, B. Lamontagne, and J. H. Schmid, "Spiral-path high-sensitivity silicon photonic wire molecular sensor with temperature-independent response," *Opt. Lett.*, vol. 33, no. 6, pp. 596–598, Mar. 2008.

[7] P. J. Bock, P. Cheben, J. H. Schmid, J. Lapointe, A. Delâge, S. Janz, G. C. Aers, D.-X. Xu, A. Densmore, and T. J. Hall, "Subwavelength grating periodic structures in silicon-on-insulator: A new type of microphotonic waveguide," *Opt. Express*, vol. 18, no. 19, pp. 20 251–20 262, Sep. 2010.

[8] T. Barwicz and H. Haus, "Three-dimensional analysis of scattering losses due to sidewall roughness in microphotonic waveguides," *J. Lightw. Technol.*, vol. 23, no. 9, pp. 2719–2732, Sep. 2005.

[9] J. P. R. Lacey and F. P. Payne, "Radiation loss from planar waveguides with random wall imperfections," *Proc. Inst. Elect. Eng.—J. Optoelectron.*, vol. 137, no. 4, pp. 282–288, Aug. 1990.

[10] W. Bogaerts, P. Dumon, D. Van Thourhout, and R. Baets, "Low-loss, low-cross-talk crossings for silicon-on-insulator nanophotonic waveguides," *Opt. Lett.*, vol. 32, no. 19, pp. 2801–2803, Oct. 2007.

[11] P. Sanchis, P. Villalba, F. Cuesta, A. Håkansson, A. Griol, J. V. Galán, A. Brimont, and J. Martí, "Highly efficient crossing structure for silicon-on-insulator waveguides," *Opt. Lett.*, vol. 34, no. 18, pp. 2760–2762, Sep. 2009.

[12] P. J. Bock, P. Cheben, J. H. Schmid, J. Lapointe, A. Delâge, D.-X. Xu, S. Janz, A. Densmore, and T. J. Hall, "Subwavelength grating crossings for silicon wire waveguides," *Opt. Express*, vol. 18, no. 15, pp. 16 146–16 155, Jul. 2010.

[13] P. Cheben, P. J. Bock, J. H. Schmid, J. Lapointe, S. Janz, D.-X. Xu, A. Densmore, A. Delâge, B. Lamontagne, and T. J. Hall, "Refractive index engineering with subwavelength gratings for efficient microphotonic couplers and planar waveguide multiplexers," *Opt. Lett.*, vol. 35, no. 15, pp. 2526–2528, Aug. 2010.

[14] P. Cheben, D.-X. Xu, S. Janz, and A. Densmore, "Subwavelength waveguide grating for mode conversion and light coupling in integrated optics," *Opt. Express*, vol. 14, no. 11, pp. 4695–4702, May 2006.

[15] V. R. Almeida, R. R. Panepucci, and M. Lipson, "Nanotaper for compact mode conversion," *Opt. Lett.*, vol. 28, no. 15, pp. 1302–1304, Aug. 2003.

[16] D. Taillaert, W. Bogaerts, P. Bienstmann, T. F. Krauss, P. Van Daele, I. Moerman, S. Verstuyft, K. De Mesel, and R. Baets, "An out-of-plane-grating coupler for efficient butt-coupling between compact planar waveguides and single-mode fibers," *IEEE J. Quantum Electron.*, vol. 38, no. 7, pp. 949–955, Jul. 2002.

[17] D. Taillaert, P. Bienstmann, and R. Baets, "Compact efficient broadband grating coupler for silicon-on-insulator waveguides," *Opt. Lett.*, vol. 29, no. 23, pp. 2749–2751, Dec. 2004.

[18] R. Halir, P. Cheben, S. Janz, D.-X. Xu, I. Molina-Fernández, and J. G. Wangüemert-Pérez, "Waveguide grating coupler with subwavelength microstructures," *Opt. Lett.*, vol. 34, no. 9, pp. 1408–1410, May 2009.

[19] R. Halir, P. Cheben, J. H. Schmid, R. Ma, D. Bedard, S. Janz, D.-X. Xu, A. Densmore, J. Lapointe, and I. Molina-Fernández, "Continuously apodized fiber-to-chip-surface coupler with refractive index engineered subwavelength structure," *Opt. Lett.*, vol. 35, no. 19, pp. 3243–3245, Oct. 2010.

[20] X. Chen and H. K. Tsang, "Nanoholes grating couplers for coupling between silicon-on-insulator waveguides and optical fibers," *IEEE Photon. J.*, vol. 1, no. 3, pp. 184–190, Sep. 2009.

[21] L. Liu, M. Pu, K. Yvind, and J. M. Hvam, "High-efficiency, large-bandwidth silicon-on-insulator grating coupler based on a fully-etched photonic crystal structure," *Appl. Phys. Lett.*, vol. 96, no. 5, p. 051 126, Feb. 2010.

[22] J. Feng and Z. Zhou, "Polarization beam splitter using a binary blazed grating coupler," *Opt. Lett.*, vol. 32, no. 12, pp. 1662–1664, Jun. 2007.

[23] J. Yang, Z. Zhou, X. Wang, D. Wu, H. Yi, J. Yang, and W. Zhou, "Compact double-layer subwavelength binary blazed grating 1x4 splitter based on silicon-on-insulator," *Opt. Lett.*, vol. 36, no. 6, pp. 837–839, 2011.

[24] P. J. Bock, P. Cheben, A. Delâge, J. H. Schmid, D.-X. Xu, S. Janz, and T. J. Hall, "Demultiplexer with blazed waveguide sidewall grating and subwavelength grating structure," *Opt. Express*, vol. 16, no. 22, pp. 17 616–17 625, Oct. 2008.
[25] C. Koos, P. Vorreau, T. Vallaitis, P. Dumon, W. Bogaerts, R. Baets, B. Esembeson, I. Biaggio, T. Michinobu, F. Diederich, W. Freude, and J. Leuthold, "All-optical high-speed signal processing with silicon–organic hybrid slot waveguides," *Nature Photon.*, vol. 3, no. 4, pp. 216–219, 2009.
[26] J.-M. Lee, D.-J. Kim, H. Ahn, S.-H. Park, and G. Kim, "Temperature dependence of silicon nanophotonic ring resonator with a polymeric overlayer," *J. Lightw. Technol.*, vol. 25, no. 8, pp. 2236–2243, Aug. 2007.
[27] W. N. Ye, J. Michel, and L. C. Kimerling, "Athermal high-index-contrast waveguide design," *IEEE Photon. Technol. Lett.*, vol. 20, no. 11, pp. 885–887, Jun. 2008.
[28] D. H. Spadoti, L. H. Gabrielli, C. B. Poitras, and M. Lipson, "Focusing light in a curved space," *Opt. Express*, vol. 18, no. 3, pp. 3181–3186, Jan. 2010.